

Fluorinated Electrolytes for Li-Ion Batteries: The Lithium Difluoro(oxalato)borate Additive for Stabilizing the Solid Electrolyte Interphase

Lan Xia,^{†,‡} Saixi Lee,[†] Yabei Jiang,[†] Yonggao Xia,^{*,†} George Z. Chen,^{‡,ID} and Zhaoping Liu^{*,†}

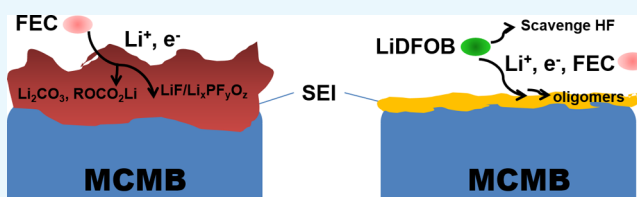
[†]Ningbo Institute of Materials Technology & Engineering (NIMTE), Chinese Academy of Sciences (CAS), Zhongguan West Road 1219, Ningbo 315201, China

[‡]Department of Chemical and Environmental Engineering, Centre for Sustainable Energy Technologies, Faculty of Science and Engineering, University of Nottingham Ningbo China, Taikang East Road 199, Ningbo 315100, China

S Supporting Information

ABSTRACT: Fluorinated electrolytes based on fluoroethylene carbonate (FEC) have been considered as promising alternative electrolytes for high-voltage and high-energy capacity lithium-ion batteries (LIBs). However, the compatibility of the fluorinated electrolytes with graphite negative electrodes is unclear. In this paper, we have systematically investigated, for the first time, the stability of fluorinated electrolytes with graphite negative electrodes, and the result shows that unlike the ethylene carbonate (EC)-based electrolyte, the FEC-based electrolyte (EC was totally replaced by FEC) is incapable of forming a protective and effective solid electrolyte interphase (SEI) that protects the electrolyte from runaway reduction on the graphite surface.

The reason is that the lowest unoccupied molecular orbital energy levels are also lowered by the introduction of fluorine into the solvent, and the FEC solvent has poorer resistance against reduction, leading to instability on the graphite negative electrode. To tackle this problem, two lithium salts of lithium bis(oxalato)borate and lithium difluoro(oxalato)borate (LiDFOB) have been investigated as negative-electrode film-forming additives. Incorporation of only 0.5 wt % LiDFOB to a FEC-based electrolyte [1.0 M LiPF₆ in 3:7 (FEC–ethyl methyl carbonate)] results in excellent cycling performance of the graphite negative electrode. This improved property originates from the generation of a thinner and better quality SEI film with little LiF by the sacrificial reduction of the LiDFOB additive on the graphite negative electrode surface. On the other hand, this additive can stabilize the electrolyte by scavenging HF. Meanwhile, the incorporated LiDFOB additive has positive influence on the interphase layer on the positive electrode surface and significantly decreases the amount of HF formation, finally leading to improved cycling stability and rate capability of LiNi_{0.5}Mn_{1.5}O₄ electrodes at a high cutoff voltage of 5 V. The data demonstrate that the LiDFOB additive not only exhibits a superior compatibility with graphite but also improves the electrochemical properties of high-voltage spinel LiNi_{0.5}Mn_{1.5}O₄ positive electrodes considerably, confirming its potential as a prospective, multifunctional additive for 5 V fluorinated electrolytes in high-energy capacity lithium-ion batteries (LIBs).



1. INTRODUCTION

Developing a new generation of 5 V-class nonaqueous electrolytes with high cathodic/anodic stability and compatibility is of great technological importance for high-voltage and high-energy capacity lithium-ion batteries.^{1,2} In this technology development, various novel electrolyte solvents and additives have been widely explored in the past decades,^{3–9} and among them, fluorinated solvents have attracted particular attention because of their high oxidation stability, low melting point, and high flash point.^{10–17} Some partially fluorinated carbonates were reported by Zhang et al.,¹⁶ who used them and a highly fluorinated ether as cosolvents and formulated fluorinated electrolytes for the 5 V-class chemistry. The results found that these fluorinated electrolytes had high resistance against oxidation, and full lithium-ion cells of LiNi_{0.5}Mn_{1.5}O₄/Li₄Ti₅O₁₂ that assembled these electrolytes showed significantly improved cycling stability. Recently, Markevich et al.¹⁷

investigated the use fluoroethylene carbonate (FEC) as a cosolvent instead of the most commonly used ethylene carbonate (EC) in LiCoPO₄/Li, LiCoPO₄/Si, and LiNi_{0.5}Mn_{1.5}O₄/Si cells; the cells using the FEC-based electrolyte exhibited better capacity retention compared with the cells containing the EC-based electrolyte. The oxidation stability of the FEC-based electrolyte was further confirmed by Hu et al.^{13,15} It is well-known that fluorine substitution in organic solvents lowers the highest occupied molecular orbital energy levels, resulting in higher oxidation stability. In the above-mentioned reports, the fluorinated electrolytes based on fluorinated solvents indicate excellent voltage stability on the high-voltage LiNi_{0.5}Mn_{1.5}O₄ and LiCoPO₄ positive electrode.

Received: August 20, 2017

Accepted: October 31, 2017

Published: December 7, 2017

However, because the lowest unoccupied molecular orbital energy levels are also lowered by the introduction of fluorine into the solvent, the fluorinated electrolytes have poorer resistance against reduction, leading to instability on graphite negative electrodes.^{16,18} In Shen et al.'s work,¹⁹ they reported the solid electrolyte interphase (SEI) layer on highly ordered pyrolytic graphite (HOPG) in two electrolytes using in situ atomic force microscopy (AFM) techniques and found that the SEI layer formed by a FEC/dimethyl carbonate (DMC)-based electrolyte was thick and dense compared to the SEI layer formed by a EC/DMC-based electrolyte. Unfortunately, the electrochemical stability of graphite negative electrodes in FEC-based electrolytes has not been reported.

In our previous works, we found that the F-electrolyte containing a new fluorinated ether, 1,1,1,3,3,3-hexafluoroisopropyl methyl ether (HFPM), as a cosolvent has good compatibility with graphite negative electrodes.²⁰ The reason is that HFPM has a high reduction potential around 1.2 V, which is beneficial for forming an effective SEI on the graphite negative electrode surface, resulting in enhanced stability on the negative side of high-voltage mesocarbon microbead (MCMB)/LiNi_{0.5}Mn_{1.5}O₄ 18 650 batteries. However, the fluorinated ether HFPM has an extremely low boiling point (50 °C) slightly above room temperature, and its boiling point is not acceptable.^{21,22} Moreover, it has a high cost in manufacturing and purification. Thus, the HFPM is not suitable as a cosolvent for high-voltage electrolytes in practice.

On the other hand, electrolyte functional additives have been developed to promote the formation of a protective SEI film on graphitic materials.^{23–27} In general, these additives are often consumed and intended for the formation of the SEI film in the initial cycles of the battery. For instance, propylene carbonate (PC) can easily reduce on graphite and co-insert with a Li ion into the interlayer structure of graphite negative electrodes, resulting in the destruction of the inner layer of graphite negative electrodes. To solve this problem, many film-forming additives including ethylene sulfite and vinyl sulfones have been reported.^{25,28–30} Prior to the electrochemical reduction of the electrolyte solvents, these additives are preferably reduced to facilitate the formation of an effective SEI on the graphite surface, which successfully prevents the cointercalation of PC molecules into graphite. In the case of the FEC-based electrolyte, the reduction of FEC starts at ca. 1.5 V versus Li⁺/Li.^{19,26} If functional additives in the electrolyte are reduced prior to this potential and are capable of forming a protective and conductive SEI, they will prevent continuous reductive decomposition, leading to an improved performance of the battery. Some prevalent lithium salts, such as lithium bis(oxalato)borate (LiBOB)³¹ and lithium difluoro(oxalato)borate (LiDFOB),³² greatly improve the SEI durability on graphite negative electrodes. Moreover, we found that these lithium salt additives can be reduced at ca. ~1.6 V and form a robust protective SEI film on the graphite surface with very low interfacial impedance. For this reason, in this paper, we introduced LiBOB and LiDFOB as film-forming additives in the FEC-based high-voltage electrolyte to alleviate its compatibility with graphite negative electrodes, discussed a systematic investigation of the influence of these additives on the performance of high-voltage LiNi_{0.5}Mn_{1.5}O₄ positive electrodes, and finally proposed an improved mechanism of the additives on the carbon negative surface.

2. RESULTS AND DISCUSSION

We all know that graphite-based negative electrodes, because of its low delithiation/lithiation potentials (<0.3 V vs Li⁺/Li), high energy capacity, and low cost, are widely used in commercial lithium-ion batteries. The FEC-based electrolytes show excellent cycling stability on the high-voltage LiNi_{0.5}Mn_{1.5}O₄ and LiCoPO₄ positive electrodes. However, the electrochemical stability of graphite negative electrodes in FEC-based high-voltage electrolytes has not been reported. To clarify the electrochemical compatibility of the FEC-based high-voltage electrolyte with graphite negative electrodes, we examined the discharge–charge properties of Li/MCMB coin cells in these electrolytes by galvanostatic testing. The FEC-based electrolytes assembled were as follows: 1 M LiPF₆/FEC and 1 M LiPF₆/FEC–ethyl methyl carbonate (EMC) (5:5 or 4:6 or 3:7, by vol). All electrodes were cycled between 0 and 2 V at 50 mA g⁻¹. From Figure 1, it can be clearly seen that the Li/MCMB

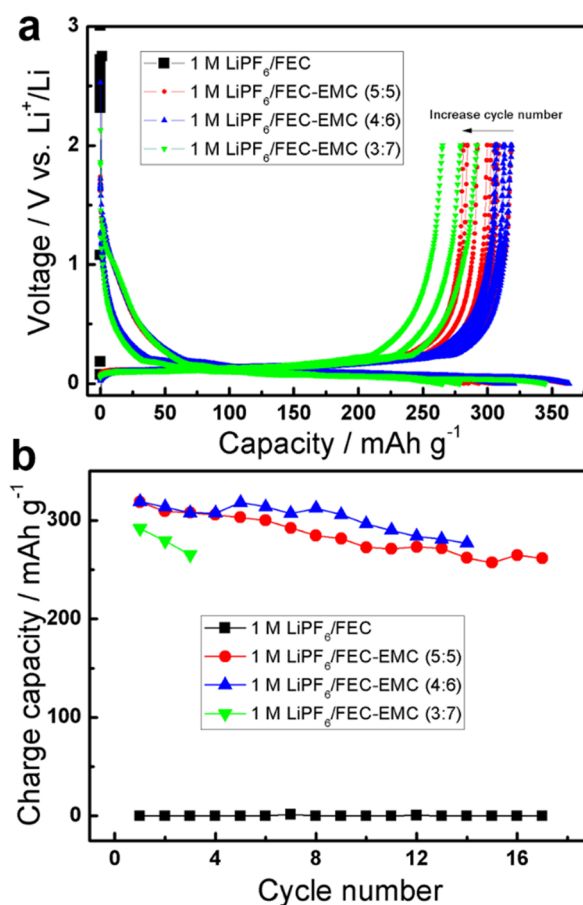


Figure 1. (a) Galvanostatic charge–discharge profiles of the Li/MCMB half cells between 0 and 2 V at 50 mA g⁻¹ in the FEC-based electrolytes. (b) Cycling behaviors of the Li/MCMB half cells assembling the FEC-based electrolytes containing various volume ratios of FEC and EMC.

cells in the 1 M LiPF₆/FEC electrolyte are hardly discharged with the discharging voltage suddenly down to the lower limit of 0 V or charged with the charging voltage steeply up to the upper limit of 2 V, showing a negligible capacity of ~0 mAh g⁻¹. The result clearly indicates the incompatibility of the 1 M LiPF₆/FEC electrolyte solution with graphite. To clarify the reason for the incompatibility of the 1 M LiPF₆/FEC electrolyte solution with graphite, we tested some experiments

about the electrolyte 1 M LiPF₆/FEC. First, we tested the ionic conductivity of the electrolytes at 25 °C. As shown in Table S1, the ionic conductivity of the electrolyte 1 M LiPF₆/FEC at room temperature still can reach 4.26 mS cm⁻¹, which is lower than that of the electrolyte 1 M LiPF₆/FEC + EMC (3/7, v/v) of ~8.88 mS cm⁻¹. This result displayed that the little high viscosity of the electrolyte 1 M LiPF₆/FEC still had a good conductivity. Second, to further eliminate the influence of the little high viscosity of the 1 M LiPF₆/FEC solution, we also tested the discharge–charge curves of Li/MCMB half coin cells in the electrolyte 1 M LiPF₆/FEC at very low currents of 20 and 5 μA. Meanwhile, to ensure the reproducibility of the result, we assembled three coin cells at a time and simultaneously tested their discharge–charge performance under the same condition. From Figure S1, we found that the discharge and charge curves of Li/MCMB cells in the 1 M LiPF₆/FEC electrolyte at a current of 20 μA were very poor. When the current was 5 μA, in the first case, there was a long plateau at about 0.2 V, and the cell was always discharged. As a result, no charge capacity can be obtained. The main reason seems to be that the stable SEI film in the FEC-based electrolyte was not well-formed in the first cycle. Additionally, Figure S2 showed the Li plating and stripping behavior in the electrolyte 1 M LiPF₆/FEC, which is in good agreement with the result reported from the literature.³⁴ Corroborating the conductivity, discharge–charge, and cyclic voltammetry (CV) results, we inferred that FEC cannot form a stable SEI film on the graphite surface, which leads to a bad cycling performance of the graphite in the 1 M LiPF₆/FEC electrolyte.

However, when the EMC cosolvent is added to the electrolytes, the cell assembling the electrolyte 1 M LiPF₆/FEC–EMC (5:5 or 4:6 or 3:7, by vol) exhibits a relatively high reversible capacity of ~310 mA h g⁻¹ at first cycle but its capacity slowly falls down to 270 mA h g⁻¹ in the subsequent 10 cycles, suggesting that although the EMC cosolvent improves the cycling performance of the cell in the FEC-based electrolytes, the MCMB electrode also exhibits an instability in the cycling performance in the FEC-based electrolyte. The galvanostatic discharge–charge curves for different cycles shown in Figure 1a further confirm the incompatibility of this electrolyte with graphite negative electrodes, which may be attributed to the fact that FEC has higher reduction potential compared to its nonfluorinated counterpart EC. Moreover, these results demonstrate that the FEC-based electrolyte is incapable of forming an effective SEI on the MCMB negative electrode surface. This conclusion is in accordance with recently reported results.¹⁹ In Shen et al.'s work,¹⁹ they studied the SEI layer on HOPG in EC- and FEC-based electrolytes using in situ AFM techniques and found that the SEI layer formed by the FEC/DMC-based electrolyte was thick and dense compared to that formed by the EC/DMC-based electrolyte.

To improve the stability of the SEI film, two film-forming additives such as LiBOB and LiDFOB were introduced into the FEC-based electrolyte. In this work, we select the 1 M LiPF₆/FEC–EMC (3:7, v/v) electrolyte as a studied FEC-based electrolyte. Furthermore, it is of importance to study the stability with lithium metal in the electrolyte because the properties of the lithiated MCMB are similar to those of lithium metal. Thus, it is meaningful to test the compatibilities of lithium metal with the FEC-based electrolytes. Figure 2 shows two photographs of the FEC-based electrolytes without and with a Li sheet after being stored for 10 days (a) and 6 months (b)

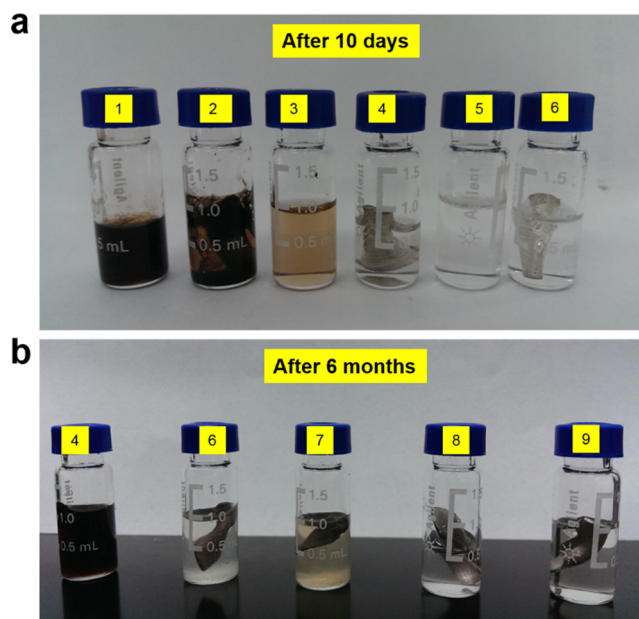
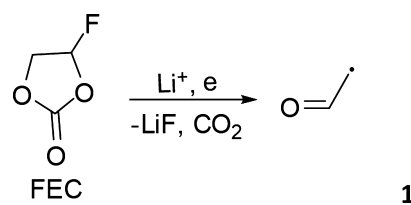


Figure 2. Photographs of the FEC-based electrolytes (1) 1 M LiPF₆/FEC, (2) 1 M LiPF₆/FEC + Li sheet, (3) 1 M LiPF₆/FEC–EMC (3:7, v/v), (4) 1 M LiPF₆/FEC–EMC (3:7, v/v) + Li sheet, (5) 1 M LiPF₆/FEC–EMC (3:7, v/v)-1 wt % LiBOB, (6) 1 M LiPF₆/FEC–EMC (3:7, v/v)-1 wt % LiBOB + Li sheet, (7) 1 M LiPF₆/FEC–EMC (3:7, v/v)-0.5 wt % LiBOB + Li sheet, (8) 1 M LiPF₆/FEC–EMC (3:7, v/v)-1 wt % LiDFOB + Li sheet, and (9) 1 M LiPF₆/FEC–EMC (3:7, v/v)-0.5 wt % LiDFOB + Li sheet after being stored for 10 days (a) and 6 months (b) in the Ar-filled glovebox at 25 °C.

(b) at 25 °C. The FEC-based electrolyte solutions are as follows: (1) 1 M LiPF₆/FEC, (2) 1 M LiPF₆/FEC + Li sheet, (3) 1 M LiPF₆/FEC–EMC (3:7, v/v), (4) 1 M LiPF₆/FEC–EMC (3:7, v/v) + Li sheet, (5) 1 M LiPF₆/FEC–EMC (3:7, v/v)-1 wt % LiBOB, (6) 1 M LiPF₆/FEC–EMC (3:7, v/v)-1 wt % LiBOB + Li sheet, (7) 1 M LiPF₆/FEC–EMC (3:7, v/v)-0.5 wt % LiBOB + Li sheet, (8) 1 M LiPF₆/FEC–EMC (3:7, v/v)-1 wt % LiDFOB + Li sheet, and (9) 1 M LiPF₆/FEC–EMC (3:7, v/v)-0.5 wt % LiDFOB + Li sheet. As shown in Figure 2a, after being stored in an Ar glovebox for 10 days, the color of the electrolytes (1) and (2) (1 M LiPF₆/FEC without/with a Li sheet) turns black. We think that the color change of the electrolyte (1) may be due to the traces of water, moisture, and alcohol resulting in the formation of hydrofluoric acid HF, which correspondingly leads to a severe deterioration of the electrolyte (1). Meanwhile, the color change of the electrolyte (2) may also be attributed to the reduction decomposition of FEC (reaction 1)³⁵ to the reaction products dissolved in the electrolyte. This result follows the conclusions reached in the previous studies.^{35,36}



By contrast, when either the Li sheet or the LiBOB additive is added in the 1 M LiPF₆/FEC–EMC (3:7) electrolyte solution, the color of the electrolytes (4–6) is still clear,

suggesting that the Li sheet and LiBOB can stabilize the FEC-based electrolyte during this short time, which may be attributed to the suppression of HF generation.³⁷ However, after 6 months, it can clearly be seen from Figure 2b that the electrolytes having no additive (4) and LiBOB (6, 7) shows a color change from dark brown to light brown, respectively. By contrast, the color of the electrolytes containing the LiDFOB additives (8, 9) is nearly unchanged after standing for 6 months, illustrating that merely 0.5 wt % LiDFOB-contained FEC-based electrolyte is stable toward lithium metal. According to the results of previous studies, the reduction potential of LiDFOB molecules is slightly higher than that of LiBOB molecules, indicating that LiDFOB will be prone to be reduced at the Li metal surface first.³² The reduction of the LiDFOB additive results in the formation of more complicated and stable oligomers to yield a passivating SEI film on the Li metal surface. Therefore, LiDFOB could be used as a film-forming additive for the FEC-based electrolyte.

To examine the anodic behavior of the FEC-based electrolytes 1 M LiPF₆/FEC–EMC (3:7, v/v) without and with the LiDFOB additive, the initial linear sweep voltammogram curves of these electrolytes using a Pt microelectrode at a scan rate of 5 mV s⁻¹, together with those of the electrolyte 1 M LiPF₆/FEC for comparison, are shown in Figure S3 (Supporting Information). As shown in Figure S3, the anodic current of the electrolyte 1 M LiPF₆/FEC starts to rise from 2.7 V versus Li⁺/Li and becomes huge at ca. 2.0 V, which is in agreement with the earlier data.²⁶ This result indicates that FEC is prone to be reduced at a higher potential. By contrast, in the first negative scan of the electrolyte 1 M LiPF₆/FEC–EMC (3:7, v/v), the huge reduction peaks at ca. 2.0 V disappear and then two weak reduction peaks emerge at 1.5 and 0.7 V, which are related to the reductive decomposition of FEC and EMC, respectively.²⁰ As for the electrolyte containing the LiDFOB additive, a new reductive peak arises at a potential of 2.5 V, which may be ascribed to the electrochemical reduction of LiDFOB molecules. To evidence the electrochemical compatibility of the FEC-based electrolyte containing the LiDFOB additive with the graphite negative electrode, the CV measurements of Li/MCMB coin cells using the electrolytes at a scan rate of 0.1 mV s⁻¹ are shown in Figure 3. As shown in the inset of Figure 3, in the first cycle, the MCMB negative electrode in the electrolyte with no additive displays two weak reduction peaks at 1.5 and 0.7 V, which are attributed to the decomposition of FEC and EMC, respectively. By contrast, the CV curve of the Li/MCMB cell using the electrolyte containing 0.5 wt % LiDFOB shows a strong reductive peak at around 1.6 V, which is believed to be the result of the reduction and polymerization of LiDFOB molecules.^{32,38} In addition, the peak positioned at 0.7 V disappears, indicating that the SEI film originating from the FEC-based electrolyte with the LiDFOB additive can inhibit the reduction of EMC. As shown in Figure 3, there is one main anodic/cathodic peak due to the reversible lithium insertion/extraction reactions with the active graphite negative electrode at a low potential region of 0.5–0.01 V, which is in good agreement with the previous reports.^{39,40} Moreover, we can see from Figure 3 that in the subsequent cycles, there was no obvious peak displacement, suggesting that the FEC-based electrolyte containing 0.5 wt % LiDFOB shows a good electrochemical compatibility with the graphite negative electrode. These CV features also suggest that LiDFOB is capable of forming a stable SEI on the graphite negative

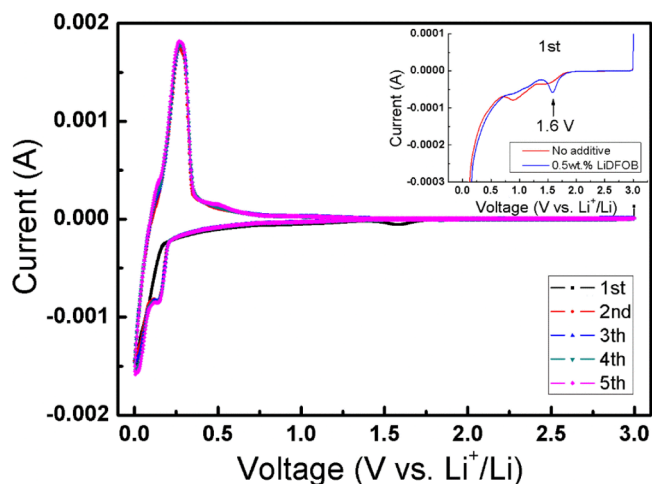


Figure 3. Typical CV curves of Li/MCMB half coin cells in the electrolyte containing 0.5 wt % LiDFOB additive. The initial CV curves of the Li/MCMB half coin cells in the FEC-based electrolyte without and with the LiDFOB additive are expressed in the inset (scan rate: 0.1 mV s⁻¹).

electrode surface to enhance the compatibility of the FEC-based electrolyte with graphite.

The discharge–charge performance of the Li/MCMB cells with the FEC-based electrolyte containing 0.5 wt % LiDFOB additive is shown in Figure 4. All electrodes were cycled at 50

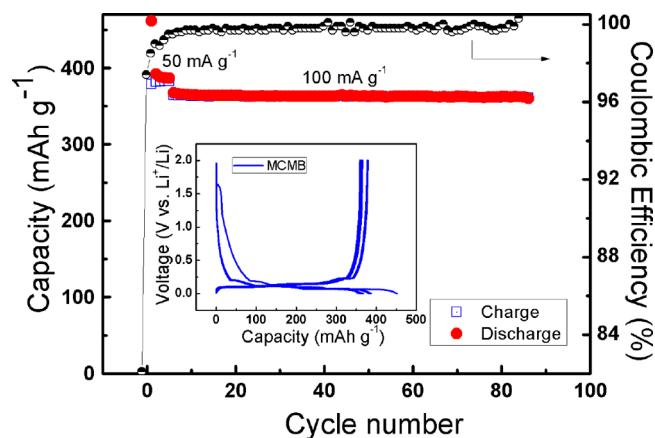


Figure 4. Curves of discharge–charge capacity and Coulombic efficiency vs cycle number obtained upon galvanostatic cycling for Li/MCMB coin cells in the FEC-based electrolyte containing 0.5 wt % LiDFOB additive. The inset of this figure displays the discharge–charge curves of the electrode in this electrolyte.

mA g⁻¹ in the first five cycles and at 100 mA g⁻¹ for the later cycles and a cutoff voltage of 2.0–0 V. Note that the MCMB negative electrode exhibits a high charge capacity of 373 mAh g⁻¹ and a slightly low Coulombic efficiency of 82.1% in the initial cycle, which is lower than that without the LiDFOB electrolyte (86.5%). This may be due to the SEI layer formation produced by the LiDFOB reductive decomposition on the MCMB negative electrode as shown below. After 90 cycles, the cell can still reach 362 mAh g⁻¹, corresponding to the capacity retention of 99.2% with respect to its sixth cycle at the same current density. At the same time, the Coulombic efficiency during cycling remains relatively stable (at >99%) in the 0.5 wt % LiDFOB electrolytes. Besides, the galvanostatic discharge–

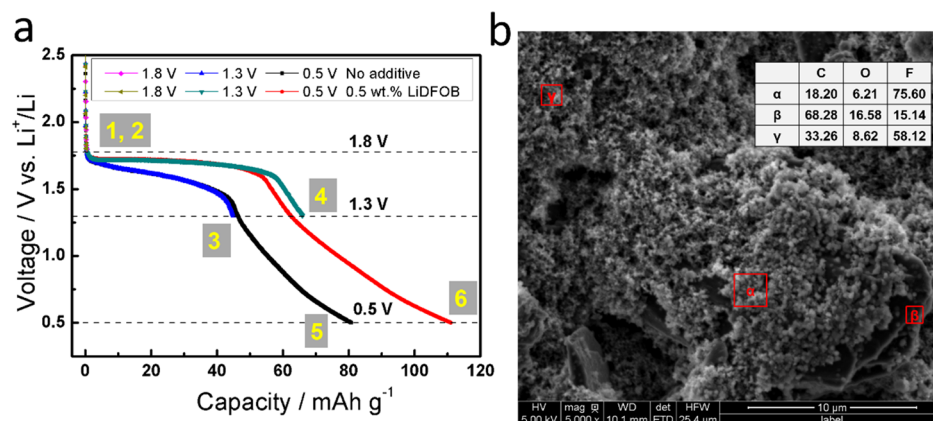


Figure 5. (a) Voltage vs capacity plots for the Li/MCMB half coin cells discharged to different cutoff voltages during first lithiation in the FEC-based electrolyte without and with the LiDFOB additive at a constant low current of $5 \mu\text{A}$. (b) SEM image of the graphite negative electrodes discharged to 0.5 V in no-additive electrolyte 1 M $\text{LiPF}_6/\text{FEC-EMC}$ (3:7, v/v). The inset of (b) shows the element composition detected by EDXS. The red squares indicate the locations probed by EDXS.

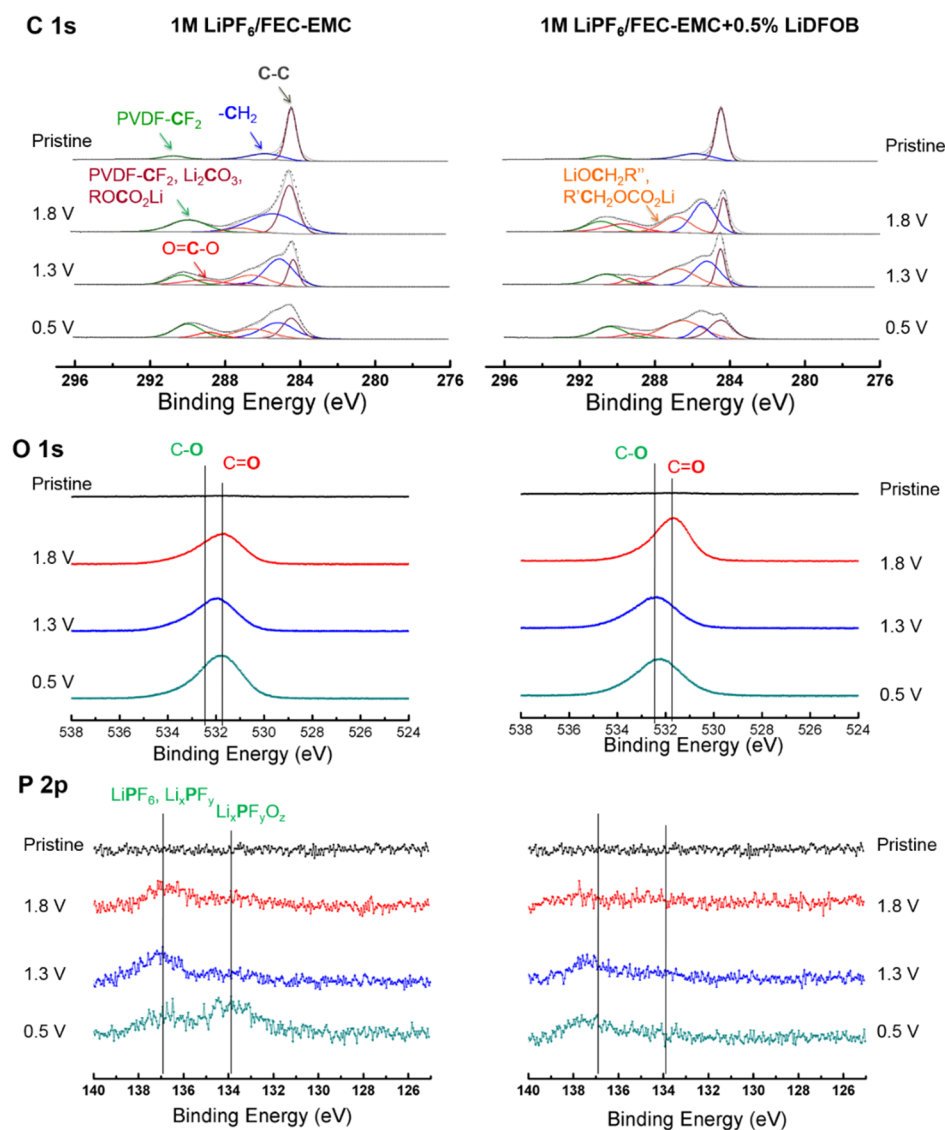


Figure 6. C 1s, O 1s, and P 2p core-level XPS spectra for MCMB electrodes before and after being discharged at 1.8, 1.3, and 0.5 V in 1 M $\text{LiPF}_6/\text{FEC-EMC}$ without and with the LiDFOB additive.

charge curves for different cycles shown in the inset of Figure 4 further confirm an excellent cycling performance of the MCMB electrode in 0.5 wt % LiDFOB electrolytes. These data suggest that the introduction of 0.5 wt % LiDFOB in the FEC-based electrolyte can obviously enhance the cycling stability of the MCMB electrode.

Different evolutions of the SEI film formed on the MCMB negative electrode in the FEC-based electrolyte without and with the LiDFOB additive have been discussed below by scanning electron microscopy (SEM), energy-dispersive X-ray spectroscopy (EDXS), and X-ray photoelectron spectroscopy (XPS). It is generally known that the first discharge data directly display the formation of the SEI film by reductive decomposition of the electrolytes. Therefore, the first discharge profile of Li/MCMB half coin cells discharged to different cutoff voltages in these two electrolytes at a constant low current of 5 μ A is shown in Figure 5a. As seen from Figure 5a, a plateau in a slope potential range of ca. 1.5 V versus Li⁺/Li attributed to the reduction of the FEC solvent was observed for the cell using the FEC-based electrolyte without an additive. However, a new plateau emerged at about 1.7 V versus Li⁺/Li for the cell with the LiDFOB additive, which is in accordance with the CV results in Figure 3. This plateau is ascribed to the reduction and polymerization of LiDFOB on the surface of the MCMB negative electrode, which results in the formation of a stable SEI on the graphite negative electrode. SEM images of MCMB surface after first discharged to 1.8, 1.3, and 0.5 V with these two electrolytes are presented in Figure S4 (Supporting Information). It can be seen from Figure S4 that when the discharged cutoff voltage was decreased successively from 1.8 to 1.3 V and further to 0.5 V, in the absence of the additive, features of pristine MCMB particles turn unclear and are difficult to be recognized, which may be due to the thick SEI film. However, in the presence of the LiDFOB additive, the surface of the graphite negative electrode is quite clean and the MCMB particles can be easily seen. This suggests that the SEI films formed on the negative electrode with the LiDFOB electrolyte in the initial cycle are thin. Moreover, we found that the surface of the negative electrode with no additive showed some white particles with low conductivity, and we speculated that these white particles might be LiF compounds, which is consistent with some experimental results and theoretical predictions in the presence of FEC.^{35,41,42} To further confirm them, the elemental concentrations of the graphite negative electrode discharged to 0.5 V in no-additive electrolyte 1 M LiPF₆/FEC–EMC (3:7, v/v) are provided in Figure 5b. The EDXS analysis shows that the concentration of the F element in the α location with more white particles is 75.6%, which is much larger than that in the β (or γ) location with no white particles, inferring that these white particles are LiF. Many LiF compounds are observed on the negative electrode surface cycled in the electrolyte without an additive, whereas the surface cycled in the LiDFOB electrolyte has not many LiF particles. The difference may be ascribed to the role of the LiDFOB additive forming a robust SEI on the negative electrode surface. On the other hand, LiDFOB can also sequester PF₅ to significantly decrease the amount of HF formation.^{37,43,44} HF severely consumes Li ions to form LiF deposited on the surface of the negative electrode.

The positive impact of the LiDFOB additive on the surface chemistry of the graphite negative electrode is confirmed by a comparison of the XPS spectra obtained from MCMB negative electrodes discharged to different cutoff voltages in the

electrolytes 1 M LiPF₆/FEC–EMC without and with the LiDFOB additive, as displayed in Figure 6. Table S2 (Supporting Information) provides the atomic concentrations (%) of the graphite negative electrode surface as determined by XPS. For these two electrolytes, the atomic concentration of C decreased while the concentration of O increased during the initial discharge, suggesting the formation of the SEI film. Additionally, we observed a small amount of B on the graphite surface discharged with the LiDFOB-containing electrolyte, which indicates that the addition of LiDFOB can modify the SEI by its reduction on the negative electrode surface. The C 1s spectrum of the pristine graphite shows three peaks. After discharged to different cutoff voltages in these two electrolytes, analysis of the MCMB negative electrode indicates new species in the C 1s, O 1s, and P 2p XPS spectra, which character the decomposition products of the electrolyte on the graphite surface.⁴⁵ Except for the peaks shown on the pristine negative electrode, the new peak at 290 \pm 0.3 eV is attributed to CO₂-like carbon from carbonate compounds such as Li₂CO₃ and/or ROCO₂Li and the other new peak at 287 \pm 0.3 eV corresponds to R₂CH₂OCO₂Li and/or LiOCH₂R.^{46,47} Their corresponding peaks for C=O and C–O are observed in the O 1s spectrum at 531.5 \pm 0.2 and 532.5 \pm 0.2 eV, respectively.^{48,49} As displayed in the C 1s and O 1s spectra in Figure 6, we can see that for the electrolyte without the LiDFOB additive, the higher relative intensity of the C=O peaks suggests that the CO₂-like compounds are the dominant components of the SEI layer, indicating much electrolyte decomposition.⁴² However, for the LiDFOB-containing electrolyte, the single-bonded carbon dominates the SEI composition. These results suggest that the addition of LiDFOB can effectively suppress the reductive decomposition of the FEC-based electrolyte. Furthermore, the P 2p spectra in Figure 6 display peaks for LiPF₆/Li_xPF_y (F–P) (at 137 \pm 0.1 eV) and Li_xPF_yO_z (F–P–O) (at 134 \pm 0.1 eV) in the SEI layer on the graphite negative electrodes discharged in these electrolytes. Li_xPF_yO_z species is originated from the LiPF₆ salt decomposition and/or hydrolysis product in the SEI layer. The intensity of the Li_xPF_yO_z peak clearly decreased in the LiDFOB-added electrolyte. This is likely because LiDFOB captures trace amounts of moisture in the electrolyte and reduces the decomposition of the salt, which is in good agreement with the results mentioned above.

Figure 7 illustrates the proposed models of the SEI structure in the FEC-based electrolyte without and with LiDFOB on the

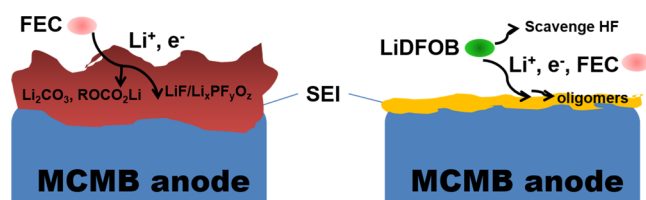


Figure 7. Proposed models of the SEI structure in the FEC-based electrolyte without and with LiDFOB on the MCMB negative electrode surface.

MCMB negative electrode surface. In the absence of the LiDFOB additive, more FEC solvents and LiPF₆ salts are reduced to form a thick, breakable SEI film having more CO₂-like compounds, Li_xPF_yO_z derivatives, and LiF on the surface of the graphite, resulting in poor cycling performance of the graphite. By contrast, incorporation of only 0.5 wt % LiDFOB to a FEC-based electrolyte [1.0 M LiPF₆ in 3:7 (FEC–EMC)]

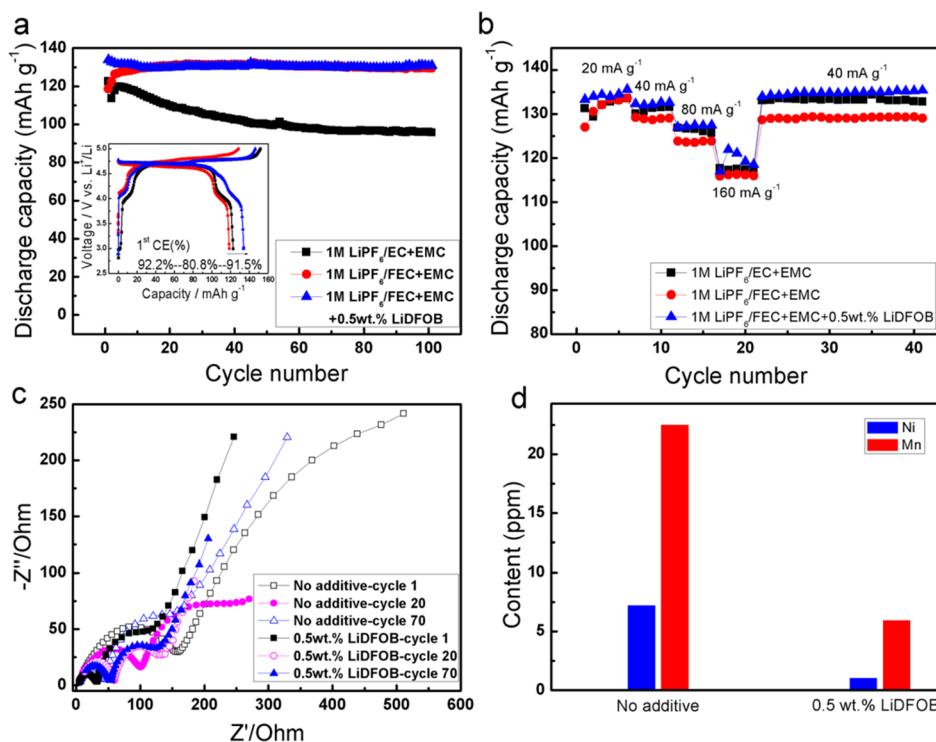


Figure 8. (a) Cycling performances of the Li/LiNi_{0.5}Mn_{1.5}O₄ cells in the electrolytes at a current density of 40 mA g⁻¹ and a cutoff voltage of 3.0–5.0 V. The inset displays the initial charge–discharge curves of the electrodes in the electrolytes. (b) Rate capabilities of the electrodes in different electrolytes. (c) Electrochemical impedance spectroscopy (EIS) curves of the Li/LiNi_{0.5}Mn_{1.5}O₄ coil cells after 1, 20, and 70 cycles with no-additive electrolyte 1 M LiPF₆/FEC–EMC (3:7, v/v) and the electrolyte containing 0.5 wt % LiDFOB additive. (d) Comparison of contents of Mn and Ni ions dissolved from LiNi_{0.5}Mn_{1.5}O₄ powders stored in these two electrolytes at 25 °C for 20 days.

results in excellent cycling performance of the graphite negative electrode. This improved property originates from the generation of a thin and robust SEI film by the sacrificial reduction of the LiDFOB additive on the graphite negative electrode surface and the stabilization of the electrolyte by scavenging HF.

Besides, to investigate the influence of the 0.5 wt % LiDFOB electrolyte on the electrochemical performance of the high-voltage positive electrodes, the high-voltage LiNi_{0.5}Mn_{1.5}O₄ positive electrode was selected and the properties of the LiDFOB additive on the positive electrode were examined. Figure 8a compares the cycling capacities of the Li/LiNi_{0.5}Mn_{1.5}O₄ cells in different electrolytes at a current density of 40 mA g⁻¹ and a cutoff voltage of 3.0–5.0 V. Although the LiNi_{0.5}Mn_{1.5}O₄ positive electrode in the EC-based electrolyte 1 M LiPF₆/EC–EMC displays a slightly high reversible capacity of 122.6 mAh g⁻¹ and a relatively low Coulombic efficiency of 80.8% at the first cycle, its capacity decreases rapidly down to 95.7 mAh g⁻¹ after 100 cycles, exhibiting a very low capacity retention of 78%. By contrast, both of the positive electrodes in the FEC-based electrolytes without and with the LiDFOB additive demonstrate a good cycling stability. Compared to the positive electrode using the FEC-based electrolyte with no additive, the positive electrode in the 0.5 wt % LiDFOB electrolyte shows a strong discharge capacity of 133.8 mAh g⁻¹ in the initial cycle and still delivers a reversible capacity of 130.9 mAh g⁻¹ at 100th cycle, showing an excellent cyclability with a capacity retention of 98%. Moreover, its initial Coulombic efficiency still reaches 91.5%, which is almost consistent with that of the electrolyte without an additive (92.2%). It can be also seen from the inset of Figure 8a that both of the positive

electrodes with the FEC-based electrolyte without and with the LiDFOB additive display similar charge–discharge profiles, where the positive electrode in the FEC electrolyte without an additive has a 50 mV higher charge voltage and a 40 mV lower discharge voltage than those in the LiDFOB electrolyte, implying that the LiDFOB additive can form a stable interface film on the LiNi_{0.5}Mn_{1.5}O₄ positive electrode with very low interfacial impedance to improve the cycling performance of the high-voltage spinel half cells. The rate capabilities of these electrodes in different electrolytes are given in Figure 8b. It can be clearly seen that the positive electrode with the LiDFOB electrolyte also exhibits a good rate capability compared with the electrode in the FEC-based electrolyte without LiDFOB. These data suggest that the LiDFOB additive is able to enhance the electrochemical performance of the high-voltage LiNi_{0.5}Mn_{1.5}O₄ positive electrode in the FEC-based electrolyte.

The effect of the LiDFOB additive can be evidenced from EIS of the Li/LiNi_{0.5}Mn_{1.5}O₄ cells using these two FEC-based electrolytes after the 1st, 20th, and 70th cycles (see Figure 8c). The results showed that all EIS spectra had two well-defined semicircles at high frequencies, representing the Li⁺-ion migration resistance (R_{SEI}) through the interphase film on the positive electrode surface and the interfacial charge-transfer resistance (R_{CT}). It can be seen from Figure 8c that the values of R_{SEI} and R_{CT} for the LiDFOB electrolyte are smaller than those for the FEC-based electrolyte without LiDFOB after the 1st, 20th, and 70th cycles, indicating that in the presence of LiDFOB, a protective interphase film with low interfacial impedance on the positive electrode surface is formed. Moreover, with increasing cycles, the R_{CT} value of the LiNi_{0.5}Mn_{1.5}O₄ electrode in the 0.5 wt % LiDFOB-containing

electrolyte remains almost at the same level, indicating that the interphase film remains stable and has no obvious change during cycling. These results were also confirmed by the SEM images of the positive electrode surfaces before and after 70 cycles in different electrolytes, as shown in Figure S6 (Supporting Information). The SEM image of the positive electrode cycled the 0.5 wt % LiDFOB electrolyte displayed a very clean surface; no degradation species precipitated on its surface. Furthermore, the amounts of Mn and Ni dissolution from the $\text{LiNi}_{0.5}\text{Mn}_{1.5}\text{O}_4$ powders in these two FEC-based electrolytes at 25 °C for 20 days are measured by inductively coupled plasma (ICP), as depicted in Figure 8d. It can be seen that 7.24 ppm of Ni ions and 22.51 ppm of Mn ions are dissolved in the FEC-based electrolyte with no additive, whereas less than 1.06 ppm of Ni ions and 5.96 ppm of Mn ions are observed in the LiDFOB-containing electrolyte, which is related to the role of LiDFOB sequestering PF_5 and resulting in a decrease in the amount of HF formation.^{37,43,44} Therefore, the decrease of dissolved Ni and Mn during storage due to the presence of the LiDFOB additive in the FEC-based electrolyte also improves the cyclability of Li/LiNi_{0.5}Mn_{1.5}O₄ coin cells, as shown in Figure 8a,b. These data indicate that the addition of 0.5 wt % LiDFOB in the FEC-based high-voltage electrolyte has positive influence on the interphase film on the positive electrode surface and significantly decreases the amount of HF formation, finally leading to excellent cycling performance of the positive electrode.

3. CONCLUSIONS

In summary, we have investigated, for the first time, the compatibility of the FEC-based electrolyte with the graphite negative electrode, and the result shows that the FEC-based electrolyte is incapable of forming a protective and effective SEI on the graphite surface, which is attributed to the fact that FEC has higher reduction potential compared to its nonfluorinated counterpart EC. To suppress the reduction of FEC, two lithium salts of LiBOB and LiDFOB have been investigated as negative-electrode film-forming additives. Incorporation of only 0.5 wt % LiDFOB to a FEC-based electrolyte [1.0 M LiPF₆ in 3:7 (FEC–EMC)] results in excellent cycling performance of the graphite negative electrode. This improved property originates from the generation of a thin and robust SEI film by the sacrificial reduction of the LiDFOB additive on the graphite negative electrode surface and the stabilization of the electrolyte by scavenging HF. Meanwhile, the incorporated LiDFOB additive has positive influence on the interphase film on the positive electrode surface and significantly decreases the amount of HF formation, finally leading to improved cycling stability and rate capability of the LiNi_{0.5}Mn_{1.5}O₄ electrode at a high cutoff voltage of 5 V. The results demonstrate that the LiDFOB additive not only exhibits a superior compatibility with graphite but also improves the electrochemical properties of the high-voltage spinel LiNi_{0.5}Mn_{1.5}O₄ positive electrode considerably, confirming its potential as a promising, multi-functional additive for 5 V fluorinated electrolytes in high-energy capacity lithium-ion batteries.

4. EXPERIMENTAL SECTION

Li-battery-grade EMC (purity 99.99%, H₂O ≤ 10 ppm) and lithium salts including lithium hexafluorophosphate (LiPF₆, purity 99.95%, H₂O ≤ 20 ppm), LiBOB (purity 99.9%, H₂O ≤ 20 ppm), and LiDFOB (purity 99.9%, Cl ≤ 15 ppm, H₂O ≤ 20

ppm) were purchased from Zhangjiagang Guotai Huarong New Chemical Materials Co. Ltd, China, and used without any additional purification process. The solvent FEC was obtained from BASF SE (purity 99.9%, H₂O ≤ 10 ppm). We also made some checks by Karl Fischer titration to determine the water content of EMC and FEC solvents. The result showed that the contents of water in the EMC and FEC solvents are 5 and 8 ppm, respectively. The electrolytes used in this work were prepared in an argon-filled glovebox with an oxygen level and a water level below 5 ppm. The EC-based electrolyte was a mixture of 1.0 M LiPF₆ dissolved in EC–EMC (3:7 by volume). All salts and solvents were used without further purification. All prepared and obtained electrolytes were stored in an argon-filled glovebox at room temperature. High-voltage positive electrode material spinel LiNi_{0.5}Mn_{1.5}O₄ powder was synthesized via solid-state reaction as reported elsewhere.³³ The positive electrode was composed of 80 wt % active materials, 10 wt % Super P carbon black, and 10 wt % poly(vinylidene fluoride) (PVDF). The graphite negative electrode consisted of 85 wt % MCMB powders, 7 wt % Super P, and 8 wt % PVDF.

The ion conductivity of the electrolytes was measured on a DDS-307 (INESA Scientific Instrument Co., Ltd, Shanghai, China) at 25 °C. The Li plating and stripping behavior in the electrolyte 1 M LiPF₆/FEC was measured by CV experiments. CV curves were tested on Solartron 1470E multichannel potentiostats using a three-electrode electrochemical cell with a Pt disc of 2 mm diameter as a working electrode and Li sheet as both reference electrode and counter electrode. The scan rate was 50 mV s⁻¹. To examine the anodic behavior of the FEC-based electrolytes without and with an additive, their initial linear sweep voltammograms were carried out on Solartron 1470E multichannel potentiostats using a three-electrode electrochemical cell with a Pt disc of 0.1 mm diameter as a working electrode and Li sheet as both reference electrode and counter electrode. The scan rate was 5 mV s⁻¹. The compatibilities of lithium metal with the FEC-based electrolyte were tested by being stored in an Ar-filled glovebox for 6 months at room temperature. The color changes of the electrolyte solutions after the storage were observed and recorded by a digital camera.

The charge–discharge measurements were performed using a CR2032-type coin cell assembled in an argon-filled glovebox and carried out on a Land CT2001A battery testing system (Wuhan, China). The counter electrode and reference electrode were lithium sheets. The separator was Celgard 2400 microporous membrane. CV experiments were carried out on Solartron 1470E multichannel potentiostats using half cells in a voltage range of 0–2.0 V at a scan rate of 0.1 mV s⁻¹. After the Li/LiNi_{0.5}Mn_{1.5}O₄ coin cell is discharged to 3.0 V, the EIS measurement of the cells was conducted on an Autolab electrochemical analytical instrument (ECO CHEMIE, B. V. Utrecht, The Netherlands) with an oscillation amplitude of 5 mV at a frequency range from 10 mHz to 100 kHz.

The effects of the LiDFOB additive on the electrochemical compatibilities of the MCMB negative electrodes were investigated by comparing the first discharge curves, surface morphology, and composition of MCMB negative electrode after different cutoff voltages. Galvanostatic lithiation was performed by the first discharged to 1.8, 1.3, and 0.5 V at a constant current of 5 μA in the FEC-based electrolytes without and with the LiDFOB additive. After the electrochemical lithiation, the MCMB samples were washed with pure DMC to remove the precipitates on the electrode surface. The surface

morphology was characterized using a Phenom Pro electron microscope (Phenom-World, The Netherlands). EDXS (FESEM, S-4800, Hitachi, Japan) was used to detect the element composition at various regions on the MCMB negative electrode surface. XPS measurements were carried out using an AXIS Ultra DLD spectrometer with Al K α (1253.6 eV) radiation. The binding energy scale was calibrated from the universal hydrocarbon contamination by using the C 1s peak at 284.8 eV.

For the Ni and Mn dissolution experiments, the fresh LiNi_{0.5}Mn_{1.5}O₄ powders were, respectively, added into the fresh FEC-based electrolytes without an additive and with the LiDFOB additive and then stored in an Ar-filled glovebox at room temperature for 20 days. The amount of electrolyte was controlled to be 1 mL per 0.1 mg of LiNi_{0.5}Mn_{1.5}O₄ powders. After the storage, the LiNi_{0.5}Mn_{1.5}O₄ powders were separated by the use of a centrifuge to sample the electrolytes, and the resulting electrolytes were analyzed via ICP–atomic emission spectrometry (ICP, Optima 2100, PerkinElmer).

■ ASSOCIATED CONTENT

● Supporting Information

The Supporting Information is available free of charge on the ACS Publications website at DOI: 10.1021/acsomega.7b01196.

Composition and ionic conductivity of the electrolytes; discharge–charge curve of Li/MCMB half coin cells; cyclic voltammogram of Li plating/stripping; initial linear sweep voltammogram curves of different FEC-based electrolyte solutions; SEM images of MCMB surface after being discharged to 1.8, 1.3, and 0.5 V with the two electrolytes; atomic concentration (%) of graphite negative electrode surface as determined by XPS; XPS F 1s core-level spectra for MCMB electrodes; SEM images of the LiNi_{0.5}Mn_{1.5}O₄ positive electrodes before and after 70 cycles with different electrolytes; and Cycling performances, rate capabilities, and EIS curves of the Li/LiNi_{0.5}Mn_{1.5}O₄ cells (PDF)

■ AUTHOR INFORMATION

Corresponding Authors

*E-mail: xiayg@nimte.ac.cn (Y. Xia).

*E-mail: liuzp@nimte.ac.cn (Z. Liu).

ORCID

George Z. Chen: 0000-0002-5589-5767

Notes

The authors declare no competing financial interest.

■ ACKNOWLEDGMENTS

This work was financially supported by the National Key R&D Program of China (Grant No. 2016YFB0100100), and the National Natural Science Foundation of China (21503246), the National Science Foundation of Ningbo (2017A610022), and Strategic Priority Research Program of Chinese Academy of Sciences (CAS, XDA09010101). The authors also appreciate S. Lee (Ningbo Institute of Materials Technology & Engineering (NIMTE), Chinese Academy of Sciences) for providing the LiNi_{0.5}Mn_{1.5}O₄ powder.

■ REFERENCES

(1) Xu, K. Electrolytes and Interphases in Li-Ion Batteries and Beyond. *Chem. Rev.* **2014**, *114*, 11503–11618.

(2) Hu, M.; Pang, X.; Zhou, Z. Recent progress in high-voltage lithium ion batteries. *J. Power Sources* **2013**, *237*, 229–242.

(3) Li, C.; Zhao, Y.; Zhang, H.; Liu, J.; Jing, J.; Cui, X.; Li, S. Compatibility between LiNi_{0.5}Mn_{1.5}O₄ and electrolyte based upon lithium bis(oxalate)borate and sulfolane for high voltage lithium-ion batteries. *Electrochim. Acta* **2013**, *104*, 134–139.

(4) Duncan, H.; Salem, N.; Abu-Lebdeh, Y. Electrolyte Formulations Based on Dinitrile Solvents for High Voltage Li-Ion Batteries. *J. Electrochem. Soc.* **2013**, *160*, A838–A848.

(5) Abouimrane, A.; Belharouak, I.; Amine, K. Sulfone-based electrolytes for high-voltage Li-ion batteries. *Electrochem. Commun.* **2009**, *11*, 1073–1076.

(6) Murmann, P.; Streipert, B.; Kloepsch, R.; Ignatiev, N.; Sartori, P.; Winter, M.; Cekic-Laskovic, I. Lithium-cyclo-difluoromethane-1,1-bis(sulfonyl)imide as a stabilizing electrolyte additive for improved high voltage applications in lithium-ion batteries. *Phys. Chem. Chem. Phys.* **2015**, *17*, 9352–9358.

(7) Bouayad, H.; Wang, Z.; Dupré, N.; Dedryvère, R.; Foix, D.; Franger, S.; Martin, J.-F.; Boutafa, L.; Patoux, S.; Gonbeau, D.; Guyomard, D. Improvement of Electrode/Electrolyte Interfaces in High-Voltage Spinel Lithium-Ion Batteries by Using Glutaric Anhydride as Electrolyte Additive. *J. Phys. Chem. C* **2014**, *118*, 4634–4648.

(8) Cheng, J.-H.; Hy, S.; Rick, J.; Wang, F.-M.; Hwang, B.-J. Mechanistic Basis of Enhanced Capacity Retention Found with Novel Sulfate-Based Additive in High-Voltage Li-Ion Batteries. *J. Phys. Chem. C* **2013**, *117*, 22619–22626.

(9) Wu, F.; Zhou, H.; Bai, Y.; Wang, H.; Wu, C. Toward 5 V Li-Ion Batteries: Quantum Chemical Calculation and Electrochemical Characterization of Sulfone-Based High-Voltage Electrolytes. *ACS Appl. Mater. Interfaces* **2015**, *7*, 15098–15107.

(10) Nanbu, N.; Takehara, M.; Watanabe, S.; Ue, M.; Sasaki, Y. Polar Effect of Successive Fluorination of Dimethyl Carbonate on Physical Properties. *Bull. Chem. Soc. Jpn.* **2007**, *80*, 1302–1306.

(11) Achiha, T.; Nakajima, T.; Ohzawa, Y.; Koh, M.; Yamauchi, A.; Kagawa, M.; Aoyama, H. Electrochemical Behavior of Nonflammable Organo-Fluorine Compounds for Lithium Ion Batteries. *J. Electrochem. Soc.* **2009**, *156*, A483–A488.

(12) Fridman, K.; Sharabi, R.; Elazari, R.; Gershinsky, G.; Markevich, E.; Salitra, G.; Aurbach, D.; Garsuch, A.; Lampert, J. A new advanced lithium ion battery: Combination of high performance amorphous columnar silicon thin film anode, 5 V LiNi_{0.5}Mn_{1.5}O₄ spinel cathode and fluoroethylene carbonate-based electrolyte solution. *Electrochem. Commun.* **2013**, *33*, 31–34.

(13) Hu, L.; Amine, K.; Zhang, Z. Fluorinated electrolytes for 5-V Li-ion chemistry: Dramatic enhancement of LiNi_{0.5}Mn_{1.5}O₄/graphite cell performance by a lithium reservoir. *Electrochem. Commun.* **2014**, *44*, 34–37.

(14) Kitagawa, T.; Azuma, K.; Koh, M.; Yamauchi, A.; Kagawa, M.; Sakata, H.; Miyawaki, H.; Nakazono, A.; Arima, H.; Yamagata, M.; Ishikawa, M. Application of Fluorine-containing Solvents to LiCoO₂ Cathode in High Voltage Operation. *Electrochemistry* **2010**, *78*, 345–348.

(15) Hu, L.; Zhang, Z.; Amine, K. Fluorinated electrolytes for Li-ion battery: An FEC-based electrolyte for high voltage LiNi_{0.5}Mn_{1.5}O₄/graphite couple. *Electrochem. Commun.* **2013**, *35*, 76–79.

(16) Zhang, Z.; Hu, L.; Wu, H.; Weng, W.; Koh, M.; Redfern, P. C.; Curtiss, L. A.; Amine, K. Fluorinated electrolytes for 5 V lithium-ion battery chemistry. *Energy Environ. Sci.* **2013**, *6*, 1806–1810.

(17) Markevich, E.; Salitra, G.; Fridman, K.; Sharabi, R.; Gershinsky, G.; Garsuch, A.; Semrau, G.; Schmidt, M. A.; Aurbach, D. Fluoroethylene Carbonate as an Important Component in Electrolyte Solutions for High-Voltage Lithium Batteries: Role of Surface Chemistry on the Cathode. *Langmuir* **2014**, *30*, 7414–7424.

(18) Achiha, T.; Nakajima, T.; Ohzawa, Y.; Koh, M.; Yamauchi, A.; Kagawa, M.; Aoyama, H. Thermal Stability and Electrochemical Properties of Fluorine Compounds as Nonflammable Solvents for Lithium-Ion Batteries. *J. Electrochem. Soc.* **2010**, *157*, A707–A712.

- (19) Shen, C.; Wang, S.; Jin, Y.; Han, W.-Q. In Situ AFM Imaging of Solid Electrolyte Interfaces on HOPG with Ethylene Carbonate and Fluoroethylene Carbonate-Based Electrolytes. *ACS Appl. Mater. Interfaces* **2015**, *7*, 25441–25447.
- (20) Xia, L.; Xia, Y.; Wang, C.; Hu, H.; Lee, S.; Yu, Q.; Chen, H.; Liu, Z. S V-Class Electrolytes Based on Fluorinated Solvents for Li-Ion Batteries with Excellent Cyclability. *ChemElectroChem* **2015**, *2*, 1707–1712.
- (21) Murata, J.; Yamashita, S.; Akiyama, M.; Katayama, S.; Hiaki, T.; Sekiya, A. Vapor Pressures of Hydrofluoroethers. *J. Chem. Eng. Data* **2002**, *47*, 911–915.
- (22) Yasumoto, M.; Yamada, Y.; Murata, J.; Urata, S.; Otake, K. Critical Parameters and Vapor Pressure Measurements of Hydrofluoroethers at High Temperatures. *J. Chem. Eng. Data* **2003**, *48*, 1368–1379.
- (23) Yan, G.; Li, X.; Wang, Z.; Guo, H.; Wang, J. Compatibility of Graphite with 1,3-(1,1,2,2-Tetrafluoroethoxy)propane and Fluoroethylene Carbonate as Cosolvents for Nonaqueous Electrolyte in Lithium-Ion Batteries. *J. Phys. Chem. C* **2014**, *118*, 6586–6593.
- (24) Ota, H.; Sakata, Y.; Inoue, A.; Yamaguchi, S. Analysis of Vinylene Carbonate Derived SEI Layers on Graphite Anode. *J. Electrochem. Soc.* **2004**, *151*, A1659–A1669.
- (25) Wrodnigg, G. H.; Besenhard, J. O.; Winter, M. Ethylene Sulfite as Electrolyte Additive for Lithium-Ion Cells with Graphitic Anodes. *J. Electrochem. Soc.* **1999**, *146*, 470–472.
- (26) Mcmillan, R.; Slegel, H.; Shu, Z. X.; Wang, W. Fluoroethylene carbonate electrolyte and its use in lithium ion batteries with graphite anodes. *J. Power Sources* **1999**, *81*–82, 20–26.
- (27) Li, L.; Zhou, S.; Han, H.; Li, H.; Nie, J.; Armand, M.; Zhou, Z.; Huang, X. Transport and Electrochemical Properties and Spectral Features of Non-Aqueous Electrolytes Containing LiFSI in Linear Carbonate Solvents. *J. Electrochem. Soc.* **2011**, *158*, A74–A82.
- (28) Jeong, S.-K.; Inaba, M.; Mogi, R.; Iriyama, Y.; Abe, T.; Ogumi, Z. Surface Film Formation on a Graphite Negative Electrode in Lithium-Ion Batteries: Atomic Force Microscopy Study on the Effects of Film-Forming Additives in Propylene Carbonate Solutions. *Langmuir* **2001**, *17*, 8281–8286.
- (29) Wagner, R.; Brox, S.; Kasnatscheew, J.; Gallus, D. R.; Amereller, M.; Cekic-Laskovic, L.; Winter, M. Vinyl sulfones as SEI-forming additives in propylene carbonate based electrolytes for lithium-ion batteries. *Electrochem. Commun.* **2014**, *40*, 80–83.
- (30) Leggesse, E. G.; Jiang, J.-C. Theoretical study of the reductive decomposition of ethylene sulfite: a film-forming electrolyte additive in lithium ion batteries. *J. Phys. Chem. A* **2012**, *116*, 11025–11033.
- (31) Xu, K.; Zhang, S.; Jow, T. R. Formation of the Graphite/Electrolyte Interface by Lithium Bis(oxalato)borate. *Electrochem. Solid-State Lett.* **2003**, *6*, A117–A120.
- (32) Chen, Z.; Liu, J.; Amine, K. Lithium Difluoro(oxalato)borate as Salt for Lithium-Ion Batteries. *Electrochem. Solid-State Lett.* **2007**, *10*, A45–A47.
- (33) Lv, Y.-Z.; Jin, Y.-Z.; Xue, Y.; Wu, J.; Zhang, X.-G.; Wang, Z.-B. Electrochemical properties of high-voltage $\text{LiNi}_{0.5}\text{Mn}_{1.5}\text{O}_4$ synthesized by a solid-state method. *RSC Adv.* **2014**, *4*, 26022–26029.
- (34) Ding, F.; Xu, W.; Chen, X.; Zhang, J.; Engelhard, M. H.; Zhang, Y.; Johnson, B. R.; Crum, J. V.; Blake, T. A.; Liu, X.; Zhang, J.-G. Effects of Carbonate Solvents and Lithium Salts on Morphology and Coulombic Efficiency of Lithium Electrode. *J. Electrochem. Soc.* **2013**, *160*, A1894–A1901.
- (35) Shkrob, I. A.; Wishart, J. F.; Abraham, D. P. What Makes Fluoroethylene Carbonate Different? *J. Phys. Chem. C* **2015**, *119*, 14954–14964.
- (36) Leung, K.; Rempel, S. B.; Foster, M. E.; Ma, Y.; del la Hoz, J. M. M.; Sai, N.; Balbuena, P. B. Modeling Electrochemical Decomposition of Fluoroethylene Carbonate on Silicon Anode Surfaces in Lithium Ion Batteries. *J. Electrochem. Soc.* **2014**, *161*, A213–A221.
- (37) Pieczonka, N. P. W.; Yang, L.; Balogh, M. P.; Powell, B. R.; Chemelewski, K.; Manthiram, A.; Krachkovskiy, S. A.; Goward, G. R.; Liu, M.; Kim, J.-H. Impact of Lithium Bis(oxalato)borate Electrolyte Additive on the Performance of High-Voltage Spinel/Graphite Li-Ion Batteries. *J. Phys. Chem. C* **2013**, *117*, 22603–22612.
- (38) Liu, J.; Chen, Z.; Busking, S.; Amine, K. Lithium difluoro(oxalato)borate as a functional additive for lithium-ion batteries. *Electrochem. Commun.* **2007**, *9*, 475–479.
- (39) Noel, M.; Suryanarayanan, V. Role of carbon host lattices in Li-ion intercalation/de-intercalation processes. *J. Power Sources* **2002**, *111*, 193–209.
- (40) Kaskhedikar, N. A.; Maier, J. Lithium Storage in Carbon Nanostructures. *Adv. Mater.* **2009**, *21*, 2664–2680.
- (41) Okuno, Y.; Ushirogata, K.; Sodeyama, K.; Tateyama, Y. Decomposition of the fluoroethylene carbonate additive and the glue effect of lithium fluoride products for the solid electrolyte interphase: an ab initio study. *Phys. Chem. Chem. Phys.* **2016**, *18*, 8643–8653.
- (42) Michan, A. L.; Parimalam, B. S.; Leskes, M.; Kerber, R. N.; Yoon, T.; Grey, C. P.; Lucht, B. L. Fluoroethylene Carbonate and Vinylene Carbonate Reduction: Understanding Lithium-Ion Battery Electrolyte Additives and Solid Electrolyte Interphase Formation. *Chem. Mater.* **2016**, *28*, 8149–8159.
- (43) Sloop, S. E.; Kerr, J. B.; Kinoshita, K. The role of Li-ion battery electrolyte reactivity in performance decline and self-discharge. *J. Power Sources* **2003**, *119*–121, 330–337.
- (44) Aurbach, D.; Markovsky, B.; Talyossef, Y.; Salitra, G.; Kim, H.-J.; Choi, S. Studies of cycling behavior, ageing, and interfacial reactions of $\text{LiNi}_{0.5}\text{Mn}_{1.5}\text{O}_4$ and carbon electrodes for lithium-ion S-V cells. *J. Power Sources* **2006**, *162*, 780–789.
- (45) Nie, M.; Chalasani, D.; Abraham, D. P.; Chen, Y.; Bose, A.; Lucht, B. L. Lithium Ion Battery Graphite Solid Electrolyte Interphase Revealed by Microscopy and Spectroscopy. *J. Phys. Chem. C* **2013**, *117*, 1257–1267.
- (46) Dedryvère, R.; Gireaud, L.; Grugeon, S.; Laruelle, S.; Tarascon, J.-M.; Gonbeau, D. Characterization of Lithium Alkyl Carbonates by X-ray Photoelectron Spectroscopy: Experimental and Theoretical Study. *J. Phys. Chem. B* **2005**, *109*, 15868–15875.
- (47) Verma, P.; Maire, P.; Novák, P. A review of the features and analyses of the solid electrolyte interphase in Li-ion batteries. *Electrochim. Acta* **2010**, *55*, 6332–6341.
- (48) Niehoff, P.; Passerini, S.; Winter, M. Interface Investigations of a Commercial Lithium Ion Battery Graphite Anode Material by Sputter Depth Profile X-ray Photoelectron Spectroscopy. *Langmuir* **2013**, *29*, 5806–5816.
- (49) Cresce, A. v.; Russell, S. M.; Baker, D. R.; Gaskell, K. J.; Xu, K. In Situ and Quantitative Characterization of Solid Electrolyte Interphases. *Nano Lett.* **2014**, *14*, 1405–1412.